An efficient method of calculating composition-dependent inter-diffusion coefficients based on compressed sensing method

Yi Qin [a], Akil Narayan [d], Kaiming Cheng [e],[**], Peng Wang [c],[b],[*]

[a] LMIB & School of Mathematical Sciences, Beihang University, Beijing, China
[b] Beijing Advanced Innovation Center for Big Data and Brain Computing, China
[c] School of Integrated Circuit Science and Engineering, Beihang University, Beijing, China
[d] Department of Mathematics, University of Utah, USA
[e] Shandong Key Laboratory for High Strength Lightweight Metallic Materials, Advanced Materials Institute, Qilu University of Technology (Shandong Academy of Sciences), Jinan 250014, China

ARTICLE INFO

ABSTRACT

Composition-dependent inter-diffusion coefficients are key parameters in many physical processes. Due to the under-determinedness of the governing diffusion equations, numerical methods either impose strict physical conditions on the samples or require a computationally onerous amount of data. To address such problems, we propose a novel inverse framework to recover the diffusion coefficients using a compressed sensing method, which in principle can be extended to alloy systems with arbitrary number of species. Comparing to conventional methods, the new approach does not impose any *priori* assumptions on the functional relationship between diffusion coefficients and concentrations, nor any preference on the locations of the samples, as long as it is in the diffused zone. It also requires much less data compared to least-squares approaches. Through a few numerical examples of ternary and quandary systems, we demonstrate the accuracy and robustness of the new method.

1. Introduction

The inter-diffusivity coefficient is the dominant parameter governing exchange of substances within various kinds of practical materials. Although it provides mesoscale insight to a wide range of material processes, reliable estimation of the inter-diffusivity coefficient is difficult due to its dependence on the alloy composition and the shortage of experimental samples.

A standard practice in computational material science is to numerically determine the inter-diffusivity from the classical Fick's second law [1]. This results in n coupled one-dimensional diffusion equations for an alloy system of $n+1$ species [2,3]:

$$\frac{\partial c_i}{\partial t} = \nabla \left(\sum_{j=1}^{n} D_{ij} \nabla c_j \right), \quad i = 1, \ldots, n, \tag{1}$$

where c_i is the concentration of species i usually obtained from the diffusion coupling technique and D_{ij} is the inter-diffusion coefficient relating the diffusion of species i to the concentration gradient of species

j, which can depend on c_i. With the $(n + 1)$-th species often selected as the solute, the inter-diffusivity matrix $\mathbf{D}_{n \times n}$ consists of n^2 unknown coefficients and two distinct frameworks have since been proposed.

The first approach is primarily based on Boltzmann-Matano analysis [4,5] and aims to solve a system of time-independent first-order linear equations. For a ternary system, the Kirkaldy-Matano method [3] generates additional $(n-1)$ diffusion paths whose common intersection point leads to extra governing equations. Later studies [6,7] seek an averaged inter-diffusivity over a certain composition range along the diffusion paths. The pseudo-binary approach [8] was proposed so that only two elements are considered in the diffusion zone. In general, those methods are computationally efficient by numerically solving as system of first-order linear equations independent of time. But their applicability is limited by stringent experimental conditions, particularly in the complex diffusion process of a multi-component system [9,10].

The second approach employs numerical inverse methods and treats inter-diffusivities as functions of composition, such as in the form of polynomials [11]. In other words, the problem of determining the inter-diffusion coefficients becomes the problem of determining their

---

* Corresponding author.
** Co-corresponding author.
E-mail addresses: chengkaimingtry@gmail.com (K. Cheng), wang.peng@buaa.edu.cn (P. Wang).

functional coefficients. With the help of an iterative numerical scheme, those coefficients are adjusted until solutions of the corresponding diffusion Eqs. (1) match the composition profile or inter-diffusion flux from experimental data within a pre-defined error criteria [11–16]. Such an approach can relax physical assumptions on the experimental samples and has been used to determine inter-diffusivities of solid solution as well as IMCs in various alloy systems [17,18]. Although such approach often takes *a priori assumption on the order of its polynomial expression to avoid overfitting or unphysical higher-order terms, there is yet any study on how to select or eliminate the order of polynomials.*

In all, effectiveness of the aforementioned approaches are largely dependent on how under-determined the coupled diffusion Eqs. (1) are. The accuracy deteriorates quickly as more unknowns are introduced with additional components to the alloy system ($n + 1 > 3$), or as the complexity of the functional relationship between inter-diffusivity and species concentrations. To address such a challenge, we propose a novel hybrid mathematical framework to estimate the inter-diffusion coefficients. We employ compressed sensing to solve an under-determined linear system for the inter-diffusivity coefficients that is prescribed by the Boltzmann-Matano equations. Details of the method is presented in section 2 and its computational efficiency, robustness and low experimental cost are demonstrated via a few examples of ternary and quandary systems in section 3. Finally, section 4 summarizes our conclusions.

2. Method

The classic Boltzmann-Matano method considers the inter-diffusivity coefficients as variables dependent on composite concentrations [5]. By denoting x_0 as the contact interface location between two species and introducing a new variable, $\lambda = (x - x_0)/\sqrt{t}$, the Boltzmann-Matano method first integrates Fick's law of diffusion (1) and thus obtains a system of ordinary differential equations:

$$\frac{1}{2t} \int_{c_i^{-\infty} \text{ or } c_i^{+\infty}}^{c_i} \left(x - x_0 \right) \mathrm{d}c_i = - \sum_{j=1}^{n} D_{ij} \nabla c_j, \quad i = 1, \ldots, n. \tag{2}$$

Here $c_i^{-\infty}$ and $c_i^{+\infty}$ are the terminal compositions of the two end members, respectively; the Matano plane x_0 can be calculated as:

$$x_0 = \frac{1}{c^+ - c^-} \int_{-\infty}^{\infty} x \frac{\partial c}{\partial x} \mathrm{d}x. \tag{3}$$

Since the diffusion coefficients are considered dependent on the concentrations $D_{ij}(c_1, \ldots, c_n)$, the new Eq. (2) enables one to extract D_{ij} from experimental data of the concentration-distance profile in metal alloys. The Boltzmann-Matano method also assumes that the alloys on both sides of the interface are semi-infinite or large enough, such that the species concentration at their extreme ends is unaffected by the transient for the entire duration of the experiment. Given that the system of ordinary differential equations is generally easier to compute numerically than the original system of partial differential Eqs. (1), the Boltzmann-Matano method proves to be both accurate and convenient. Hence we take it as the basis of our inverse framework.

In practice, experimental data are often difficult and expensive to obtain. The diffusion couple technique [19] together with electron probe micro-analysis (EPMA) is often used to obtain composition profiles. For fabricating just one diffusion couple, one should first bond two blocks of materials together and hold at certain temperatures to activate inter-diffusion at the initial interface. The annealing procedure may last from hours to days, depending on the speed of forming an inter-diffusion zone wide enough for analysis. The surface of the sample should be well polished before being subjected to EPMA. Around 50–100 sample points

are often selected in a line parallel to the direction of element diffusion within the inter-diffusion zone, and it requires several minutes for the equipment to detect the composition at each point. As a result, the experiment is time-consuming to conduct and its data is thus expensive.

Meanwhile, as additional species are incorporated in the alloy and the functional order between inter-diffusivity and concentrations increases, more samples are needed to determine the diffusion matrix **D**. As a result, the relative shortage of experimental data leads to more unknowns than equations in the Boltzmann-Matano system (2), which becomes underdetermined and the diffusion coefficients cannot be uniquely determined.

To address this problem and fully utilize the few, valuable experimental samples, we employ compressed sensing (CS) to recover the diffusion matrix. In contrast to conventional least-squares method based on the L^2-norm minimization, modern compressed sensing approach seeks to solve an underdetermined linear system by seeking the solution with the smallest ℓ^1 norm, as a convex, more computable relaxation of the smallest ℓ^0 quasi-norm solution [20–22]. Over the years, a number of numerical implementations have been developed in the scientific community including l_1-magic, *SPGL*1 and *SeDuMi* among others [23–25]. An interesting point about the theory of CS is that it generally requires random measurements. Not only is this assumption crucial to the derivation of many strong theoretical results, but also measurements at random locations seem to give better results in practice and are sought out in real applications [26].

In summary, we propose the following framework to compute the diffusion coefficients:

1. *Obtain a number of m experimental samples at locations $(x_1, \ldots, x_m)$ on the concentration-distance curve.*
2. *Substitute the samples into the Boltzmann-Matano expressions (2) and rearrange the system in the form of $\mathbf{J} = \mathscr{C}\mathbf{d}$.*

   Here $\mathbf{J}_{nm \times 1}$ is the vector representing the inter-diffusion fluxes at those sample locations, e.g. evaluations for the left-hand-side of Boltzmann-Matano expression (2); $\mathscr{C}_{nm \times n^2}$ is the value of concentration gradients (∇c_j) at the sample locations; and $\mathbf{d}_{n^2 \times 1}$ is the (unknown) vectorial form of inter-diffusivities.
3. *Construct a functional relationship between inter-diffusivities and the species concentrations with k unknown functional coefficients.*
4. *Substitute the functional relationship above into the system in Step (2).*

   Now the diffusion vector $\mathbf{d}_{n^2 \times 1}$ is rewritten as the product of a diagonal matrix of $n^2 \times k$ dimension and a vector $\mathbf{a}_{k \times 1}$ for the unknown functional coefficients:

$$\mathbf{d} = \begin{bmatrix} \boldsymbol{\phi} & \mathbf{0} & \mathbf{0} \\ \mathbf{0} & \ddots & \mathbf{0} \\ \mathbf{0} & \mathbf{0} & \boldsymbol{\phi} \end{bmatrix} \mathbf{a}. \tag{4}$$

The diagonal entry $\boldsymbol{\phi}$ is the prescribed functional relationship between diffusion coefficients and concentrations at Step (3). For example, if one chooses a 2nd-order polynomial form [11]:

$$D_{ij} = \alpha_{ij}^{(0)} + \sum_{k=1}^{n} \left(\alpha_{ij}^{(k)} c_k + \alpha_{ij}^{(n+k)} c_k^2 \right). \tag{5}$$

Here the diagonal entry and the unknown vector **a** are:

$$\boldsymbol{\phi} = \begin{bmatrix} \mathbf{I} & c_1 \mathbf{I} & \cdots & c_n \mathbf{I} & c_1^2 \mathbf{I} & \cdots & c_n^2 \mathbf{I} \end{bmatrix}, \tag{6}$$

$$\mathbf{a} = \begin{bmatrix} \mathbf{a}_1 & \mathbf{a}_2 & \cdots & \mathbf{a}_i & \cdots & \mathbf{a}_n \end{bmatrix}^{\mathrm{T}}, \tag{7}$$

$$\mathbf{a}_i = \begin{bmatrix} \alpha_{1i}^{(0)} & \alpha_{2i}^{(0)} & \cdots & \alpha_{ni}^{(0)} & \cdots & \alpha_{1i}^{(n)} & \alpha_{2i}^{(n)} & \cdots & \alpha_{ni}^{(n)} \end{bmatrix}^{\mathrm{T}}, \tag{8}$$
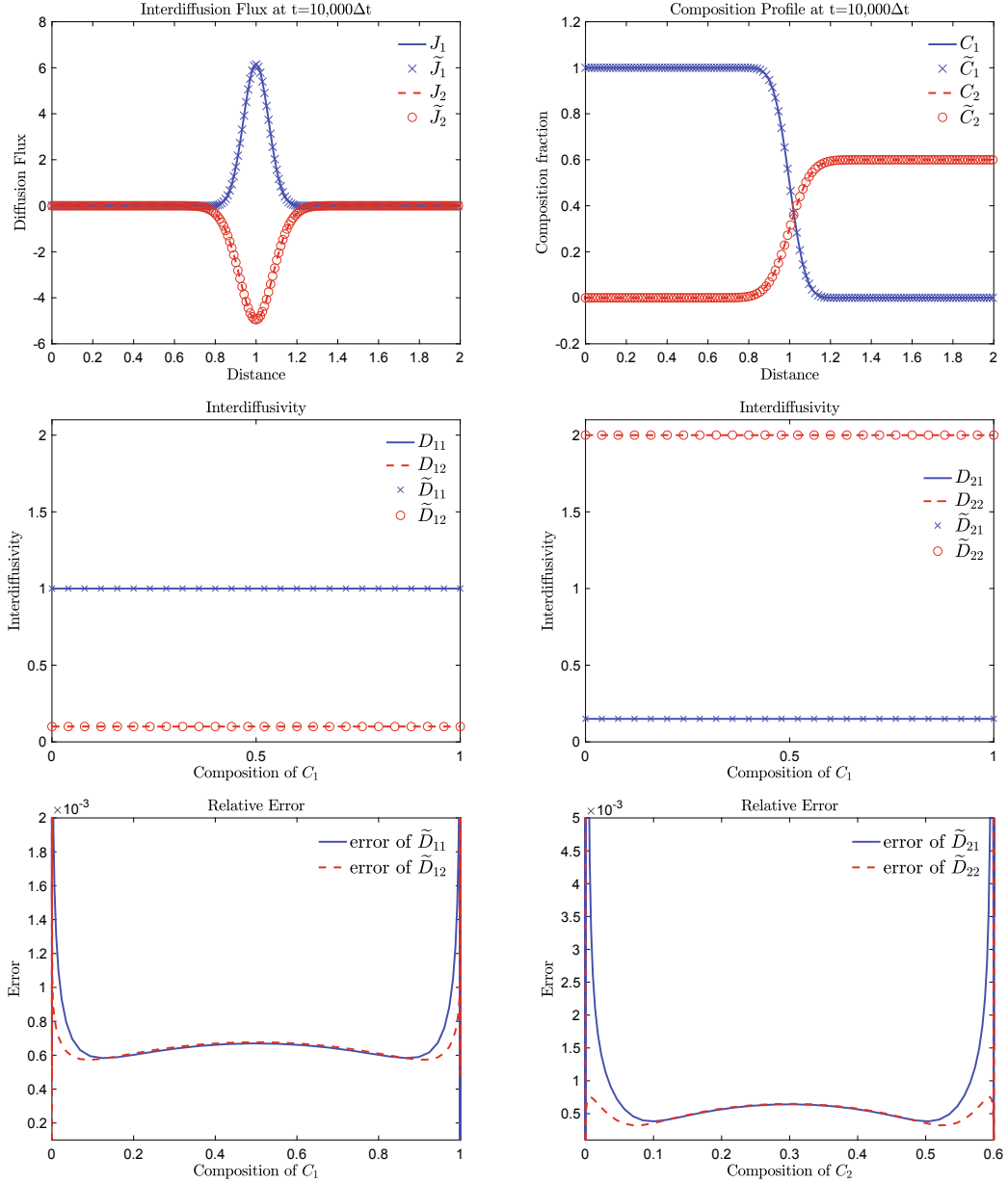
Fig. 1. Benchmark solutions and results from compressed sensing on: (a) inter-diffusion fluxes, (b) concentration profile, (c) & (d) diffusion coefficients and their relative error (10) with respect to composition (e) c_1 and (f) c_2, respectively, in the case of constant inter-diffusivities for ternary system.

where $\mathbf{I}_{n \times n}$ is the identity matrix and the superscript T represents matrix transpose.

5. *Recover the functional coefficients vector* **a** *using compressed sensing codes such as l_1-magic and SPGL1.*
6. *Recover the diffusion matrix* **D** *by substituting the computed coefficients back to the relationship in Step (3).*

It is noted here that the numerical efficiency of our method largely depends on the sparsity of the solution **a**. In addition, entries in the diffusion vector **d** are arranged by the rows and then columns from the diffusion matrix **D**,

$$\mathbf{d} = \begin{bmatrix} D_{11} & \cdots & D_{n1} & D_{12} & \cdots & D_{nn} \end{bmatrix}^{\mathrm{T}}. \quad (9)$$

Without loss of generality, our framework is applicable to arbitrary form of the diffusion-concentration relationship other than the polynomial

form (5), as long as the solution vector is sufficiently sparse. i.e., the number of non-zero entries in **a** should be at most on the same order as the number of measurements.

The error of the calculated inter-diffusivity mainly results from the deviation between computed and measured inter-diffusion flux **J** as well as concentration gradient in $\mathscr{C}$. Thus we define the relative error of each inter-diffusivity as that in an earlier study [16]:

$$\frac{\Delta D_{ij}}{\widetilde{D}_{ij}} = \sqrt{\left(\frac{J_i - \widetilde{J}_i}{\widetilde{J}_i}\right)^2 + \left(\frac{\nabla c_j - \widetilde{\nabla c_j}}{\widetilde{\nabla c_j}}\right)^2}, \quad i = 1, \dots, n; \ j = 1, \dots, n, \quad (10)$$

in which the superscript $\widetilde{A}$ represents a quantity A from the measurement data.

3. Results and discussion

In this section, we evaluate our method via a few numerical examples of ternary ($n + 1 = 3$) and quaternary ($n + 1 = 4$) systems. In each example, we assume the "true" values of the diffusion coefficients are known and the diffusion matrix is positive-definite [27]. The corresponding concentration-distance curve, computed using second-order finite difference spatial discretization and fourth-order Runge–Kutta temporal scheme in MATLAB®is considered the "benchmark" solution. As a result, data otherwise taken from experiment to extract the diffusion coefficients are now taken from arbitrary locations on those "true" solution curve, e.g. $c_i(x_0), c_i(x_1)$ and etc. In total, the data implemented in Eq. (2) include the overall diffusion time t, the measured composition c_i at the position of each analyzation point x, and the composition gradient ∇c_i, which is the slope of composition profile for each position x. To facilitate presentation, all variables are dimensionless in the examples and Δt denotes the time step. Without specification otherwise, our algorithm uses an unweighted l_1 convex optimization problem with the l_1-magic solver. Hence, for the standard "basis pursuit" problem (4), there are no tuning parameters or re/weighted ℓ_1 minimization. Finally, practical discussions on amounts of experimental data, its quality, spatial selections and the usage of our CS framework are also included at the end of this section.

3.1. Case 1: Constant Inter-diffusivity for ternary system

We validate our CS framework via a simple case of constant inter-diffusion coefficients for ternary systems ($n = 2$). Here the true inter-diffusivity matrix is set as:

$$\mathbf{D} = \begin{bmatrix} 1 & 0.1 \\ 0.15 & 2 \end{bmatrix} \tag{11}$$

Using the benchmark numerical scheme, samples at two random locations, $[c_1(x_i), c_2(x_i)], (i = 1,2)$, are taken from the concentration-distance curve at $t = 10^4 \Delta t$. Now we follow the general framework and substitute the samples into Boltzmann-Matano Eqs. (2):

$$\begin{bmatrix} \frac{\partial c_1}{\partial x}\big|_{x_1} & 0 & \frac{\partial c_2}{\partial x}\big|_{x_1} & 0 \\ 0 & \frac{\partial c_1}{\partial x}\big|_{x_1} & 0 & \frac{\partial c_2}{\partial x}\big|_{x_1} \\ \frac{\partial c_1}{\partial x}\big|_{x_2} & 0 & \frac{\partial c_2}{\partial x}\big|_{x_2} & 0 \\ 0 & \frac{\partial c_1}{\partial x}\big|_{x_2} & 0 & \frac{\partial c_2}{\partial x}\big|_{x_2} \end{bmatrix} \begin{bmatrix} D_{11} \\ D_{21} \\ D_{12} \\ D_{22} \end{bmatrix} = \begin{bmatrix} J_1\big|_{x_1} \\ J_2\big|_{x_1} \\ J_1\big|_{x_2} \\ J_2\big|_{x_2} \end{bmatrix}. \tag{12}$$

By assuming a zeroth-order functional relationship between diffusion coefficients and species concentrations, e.g. $D_{ij} = \alpha_{ij}^{(0)}$, we rewrite the expressions (4) as:

$$\mathbf{d} = \begin{bmatrix} \boldsymbol{\phi} & 0 \\ 0 & \boldsymbol{\phi} \end{bmatrix} \begin{bmatrix} \alpha_{11}^{(0)} & \alpha_{12}^{(0)} & \alpha_{21}^{(0)} & \alpha_{22}^{(0)} \end{bmatrix}^{\mathsf{T}}, \qquad \boldsymbol{\phi} = \begin{bmatrix} \mathbf{I} \end{bmatrix}, \tag{13}$$

where the identity matrix $\mathbf{I}$ is of 2×2 dimension.

Fig. 1 (a), (b), (c) & (d) plots the benchmark solutions and results from our inverse method on inter-diffusion fluxes, the concentration profile and the diffusion coefficients, respectively. As expected for such a simple case, compressed sensing provides excellent estimations. To demonstrate the robustness of our approach in the case of random samples, we took 100 pairs of samples at two arbitrary locations along the concentration-distance curve. Their ensemble average of error in terms of L_2-norm in concentration profile is as low as 10^{-5}. For a closer look, we plot the relative error of the diffusion coefficients in Fig. 1 (e) & (f). It can be seen that results become less accurate near the terminal composition than at the interface. This is a common problem when

studying composition-dependent inter-diffusivities with single diffusion coupling. The errors arise from the composition vector of the diffusion coupling lying nearly parallel to an eigenvector directions of the diffusivity matrix [28,29]. In other words, there are many more possible solutions that satisfy the terminal compositions. Although such ill-posed problem is quite trivial as terminal solutions are generally known, one can apply curve data from multiple couplings with different composition angles and describe the inter-diffusion coefficient with a single set of adjustable parameters, in order to get more reliable statistical estimation of inter-diffusivity [30].

3.2. Case 2: second-order Inter-diffusivity for ternary system

Now we consider the case in which the "true" diffusion coefficients are of second-order polynomials of concentrations in a ternary system:

$$\mathbf{D} = \begin{bmatrix} 1 - 0.1c_1 - 0.1c_2 + 0.1c_1^2 & 0.1 - 0.1c_1 + 0.1c_2 \\ 0.15 + 0.15c_1 + 0.15c_2 & 2 - 0.2c_2 - 0.2c_1 + 0.1c_2^2 \end{bmatrix}, \tag{14}$$

Now we take samples at four random locations, $[c_1(x_i), c_2(x_i)], (i = 1,...,4)$, on the "true" concentration-distance curve at $t = 8 \times 10^4 \Delta t$, obtained from the high-order numerical scheme. Substituting them into the Boltzmann-Matano Eqs. (2):

$$\begin{bmatrix} \frac{\partial c_1}{\partial x}\big|_{x_1} & 0 & \frac{\partial c_2}{\partial x}\big|_{x_1} & 0 \\ 0 & \frac{\partial c_1}{\partial x}\big|_{x_1} & 0 & \frac{\partial c_2}{\partial x}\big|_{x_1} \\ \frac{\partial c_1}{\partial x}\big|_{x_2} & 0 & \frac{\partial c_2}{\partial x}\big|_{x_2} & 0 \\ 0 & \frac{\partial c_1}{\partial x}\big|_{x_2} & 0 & \frac{\partial c_2}{\partial x}\big|_{x_2} \\ \frac{\partial c_1}{\partial x}\big|_{x_3} & 0 & \frac{\partial c_2}{\partial x}\big|_{x_3} & 0 \\ 0 & \frac{\partial c_1}{\partial x}\big|_{x_3} & 0 & \frac{\partial c_2}{\partial x}\big|_{x_3} \\ \frac{\partial c_1}{\partial x}\big|_{x_4} & 0 & \frac{\partial c_2}{\partial x}\big|_{x_4} & 0 \\ 0 & \frac{\partial c_1}{\partial x}\big|_{x_4} & 0 & \frac{\partial c_2}{\partial x}\big|_{x_4} \end{bmatrix} \begin{bmatrix} D_{11} \\ D_{21} \\ D_{12} \\ D_{22} \end{bmatrix} = \begin{bmatrix} J_1\big|_{x_1} \\ J_2\big|_{x_1} \\ J_1\big|_{x_2} \\ J_2\big|_{x_2} \\ J_1\big|_{x_3} \\ J_2\big|_{x_3} \\ J_1\big|_{x_4} \\ J_2\big|_{x_4} \end{bmatrix}. \tag{15}$$

We assume second-order polynomials for the functional relationship between diffusion coefficients and concentrations (5):

$$\begin{bmatrix} D_{11} \\ D_{21} \\ D_{12} \\ D_{22} \end{bmatrix} = \begin{bmatrix} \alpha_{11}^{(0)} + \alpha_{11}^{(1)}c_1 + \alpha_{11}^{(2)}c_2 + \alpha_{11}^{(3)}c_1^2 + \alpha_{11}^{(4)}c_2^2 \\ \alpha_{21}^{(0)} + \alpha_{21}^{(1)}c_1 + \alpha_{21}^{(2)}c_2 + \alpha_{21}^{(3)}c_1^2 + \alpha_{21}^{(4)}c_2^2 \\ \alpha_{12}^{(0)} + \alpha_{12}^{(1)}c_1 + \alpha_{12}^{(2)}c_2 + \alpha_{12}^{(3)}c_1^2 + \alpha_{12}^{(4)}c_2^2 \\ \alpha_{22}^{(0)} + \alpha_{22}^{(1)}c_1 + \alpha_{22}^{(2)}c_2 + \alpha_{22}^{(3)}c_1^2 + \alpha_{22}^{(4)}c_2^2 \end{bmatrix} = \begin{bmatrix} \boldsymbol{\phi} & 0 \\ 0 & \boldsymbol{\phi} \end{bmatrix} \begin{bmatrix} \mathbf{a}_1 \\ \mathbf{a}_2 \end{bmatrix} \tag{16}$$

Consequently, the diagonal entry (6) and $\mathbf{a}_i$ (8) become:

$$\boldsymbol{\phi} = \begin{bmatrix} \mathbf{I} & c_1\mathbf{I} & c_2\mathbf{I} & c_1^2\mathbf{I} & c_2^2\mathbf{I} \end{bmatrix}$$
$$= \begin{bmatrix} 1 & 0 & c_1 & 0 & c_2 & 0 & c_1^2 & 0 & c_2^2 & 0 \\ 0 & 1 & 0 & c_1 & 0 & c_2 & 0 & c_1^2 & 0 & c_2^2 \end{bmatrix}, \tag{17}$$

$$\mathbf{a}_i = \begin{bmatrix} \alpha_{1i}^{(0)} & \alpha_{2i}^{(0)} & \alpha_{1i}^{(1)} & \alpha_{2i}^{(1)} & \alpha_{1i}^{(2)} & \alpha_{2i}^{(2)} & \alpha_{1i}^{(3)} & \alpha_{2i}^{(3)} & \alpha_{1i}^{(4)} & \alpha_{2i}^{(4)} \end{bmatrix}^{\mathsf{T}}, \quad i = 1,2. \tag{18}$$

In Fig. 2, we compare the benchmark solutions against those from our inverse method via inter-diffusion fluxes, the concentration profile and the diffusion coefficients, respectively. Again, compressed sensing provides excellent and robust estimations. Its ensemble average L_2-form error of the concentration profile over 100 sets of four arbitrary samples remains low but rises to 10^{-3}. The relative error of the diffusion
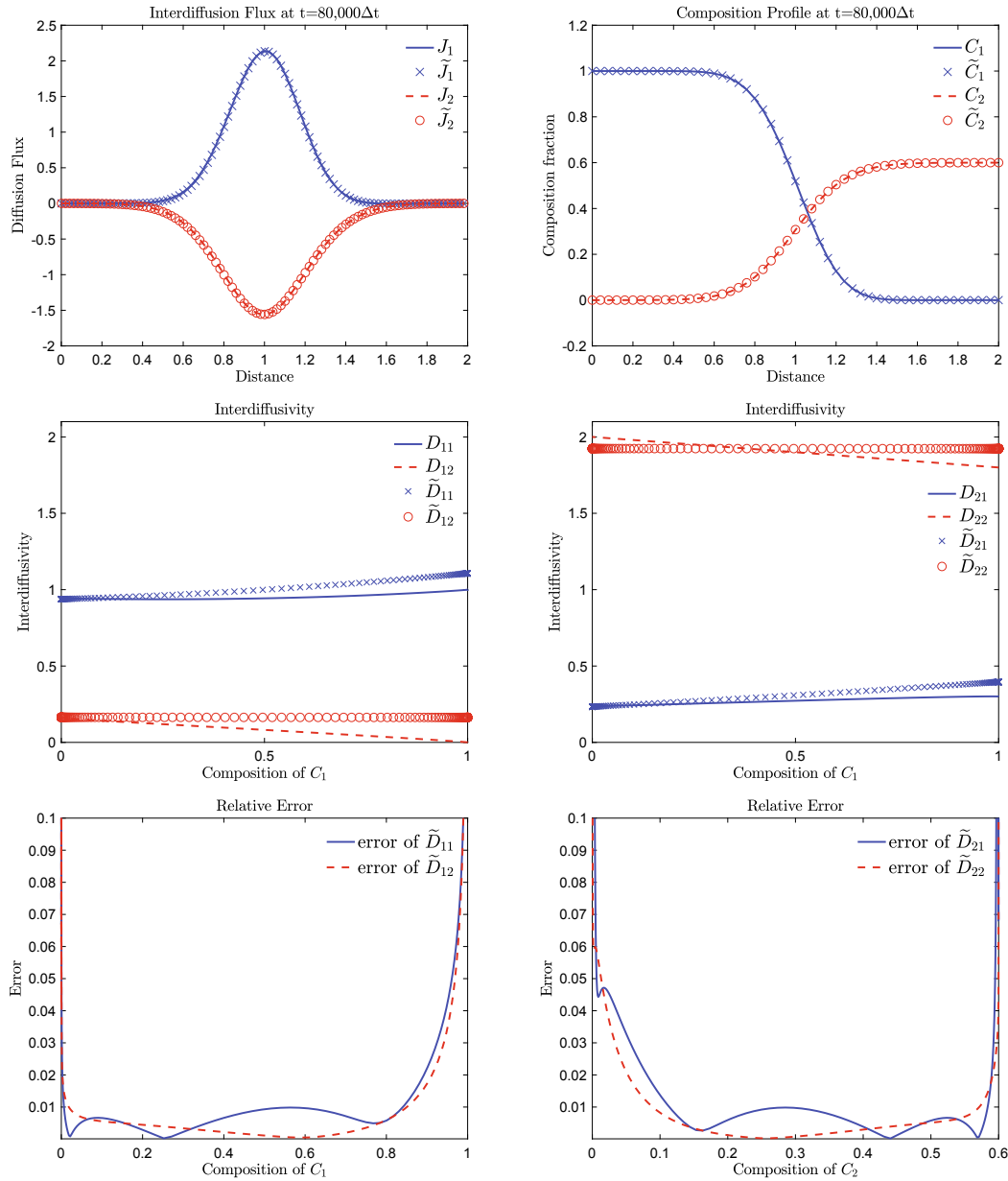
Fig. 2. Benchmark solutions and results from compressed sensing on: (a) inter-diffusion fluxes, (b) concentration profile, (c) & (d) diffusion coefficients and their relative error (10) with respect to composition (e) c_1 and (f) c_2, respectively, in the case of 2nd-order inter-diffusivities for ternary system.

coefficients are shown in Fig. 2 (e) & (f). Except those near the terminal compositions, ϵ are within 5% in most parts of the curve. We note here that the larger error at the middle range of each composition is due to larger composition gradient relative to that in the terminal region. Deviations between the computed and pre-defined inter-diffusivity may lead to misfit in the composition profiles, which is harder to detect from the composition profile. However, such misfit is exacerbated in (10) where the concentration gradient ∇c is computed and its accuracy would in turn drop in tandem with the order of derivative. Although the nature of such an inverse problem prevents one in general from obtaining the exact expressions of inter-diffusivities, one particular solution with high sparsity can be computed using CS.

3.3. Case 3: first-order Inter-diffusivity for quandary system

Lastly, we consider a quandary system ($n + 1 = 4$) whose "true" diffusion coefficients are of first-order polynomials of concentrations:

$$\mathbf{D} = \begin{bmatrix} 1 - 0.1c_1 & 0.1 & 0.2 \\ 0.05 & 2 - 0.2c_2 & 0.15 \\ 0.05 & 0.15 & 2 - 0.2c_3 \end{bmatrix}, \tag{19}$$

The corresponding "true" concentration-distance curve can be then obtained using the high-order numerical scheme and samples at four random locations, $[c_1(x_i), c_2(x_i), c_3(x_i)], (i = 1, \ldots, 4)$, are taken at $t = 8 \times 10^4 \Delta t$. Now the BM analysis (2) at those locations can be written as:

$$\begin{bmatrix} \frac{\partial c_1}{\partial x}\big|_{x_1} & 0 & 0 & \frac{\partial c_2}{\partial x}\big|_{x_1} & 0 & 0 & \frac{\partial c_3}{\partial x}\big|_{x_1} & 0 & 0 \\ 0 & \frac{\partial c_1}{\partial x}\big|_{x_1} & 0 & 0 & \frac{\partial c_2}{\partial x}\big|_{x_1} & 0 & 0 & \frac{\partial c_3}{\partial x}\big|_{x_1} & 0 \\ 0 & 0 & \frac{\partial c_1}{\partial x}\big|_{x_1} & 0 & 0 & \frac{\partial c_2}{\partial x}\big|_{x_1} & 0 & 0 & \frac{\partial c_3}{\partial x}\big|_{x_1} \\ \vdots & & & & \ddots & & & & \vdots \\ \frac{\partial c_1}{\partial x}\big|_{x_4} & 0 & 0 & \frac{\partial c_2}{\partial x}\big|_{x_4} & 0 & 0 & \frac{\partial c_3}{\partial x}\big|_{x_4} & 0 & 0 \\ 0 & \frac{\partial c_1}{\partial x}\big|_{x_4} & 0 & 0 & \frac{\partial c_2}{\partial x}\big|_{x_4} & 0 & 0 & \frac{\partial c_3}{\partial x}\big|_{x_4} & 0 \\ 0 & 0 & \frac{\partial c_1}{\partial x}\big|_{x_4} & 0 & 0 & \frac{\partial c_2}{\partial x}\big|_{x_4} & 0 & 0 & \frac{\partial c_3}{\partial x}\big|_{x_4} \end{bmatrix} \begin{bmatrix} D_{11} \\ D_{21} \\ D_{31} \\ D_{12} \\ D_{22} \\ D_{32} \\ D_{13} \\ D_{23} \\ D_{33} \end{bmatrix}$$

$$= [J_1|_{x_1} \quad J_2|_{x_1} \quad J_3|_{x_1} \quad J_1|_{x_2} \quad J_2|_{x_2} \quad J_3|_{x_2} \quad \cdots \quad J_1|_{x_4} \quad J_2|_{x_4} \quad J_3|_{x_4}]^{\mathrm{T}}. \tag{20}$$

To recover the diffusion matrix (19), we assume a first-order relationship between the diffusion coefficients and concentrations, e.g.,

$$D_{ij} = \alpha_{ij}^{(0)} + \alpha_{ij}^{(1)} c_1 + \alpha_{ij}^{(2)} c_2 + \alpha_{ij}^{(3)} c_3. \tag{21}$$

Following the proposed framework, the diffusion vector $\mathbf{d}$ (4) is expressed as:

$$\mathbf{d} = \begin{bmatrix} \boldsymbol{\phi} & \mathbf{0} & \mathbf{0} \\ \mathbf{0} & \boldsymbol{\phi} & \mathbf{0} \\ \mathbf{0} & \mathbf{0} & \boldsymbol{\phi} \end{bmatrix} \begin{bmatrix} \mathbf{a}_1 \\ \mathbf{a}_2 \\ \mathbf{a}_3 \end{bmatrix}, \tag{22}$$

with the diagonal entry (6) and $\mathbf{a}_i$ (8) ($i = 1, 2, 3$):

$$\boldsymbol{\phi} = [\mathbf{I} \quad c_1 \mathbf{I} \quad c_2 \mathbf{I} \quad c_3 \mathbf{I}], \tag{23}$$

$$\mathbf{a}_i = \begin{bmatrix} \alpha_{1i}^{(0)} & \alpha_{2i}^{(0)} & \alpha_{3i}^{(0)} & \alpha_{1i}^{(1)} & \alpha_{2i}^{(1)} & \alpha_{3i}^{(1)} & \cdots & \alpha_{1i}^{(3)} & \alpha_{2i}^{(3)} & \alpha_{3i}^{(3)} \end{bmatrix}^{\mathrm{T}}, \tag{24}$$

in which $\mathbf{I}$ is the 3×3 identity matrix.

As shown in Fig. 3 (a) & (b), the compressed sensing provides good estimates of the inter-diffusion fluxes and concentration profiles. The

ensemble average of L_2-form error in the concentration profiles, over 100 sets of four random samples, are in the range $10^{-3} \sim 10^{-2}$. However, the recovery of the diffusion coefficients deteriorates in Fig. 3 (c), (d), (e), (f), (g) & (h). Similar to their counterparts in case 1 and 2, the poor performances at terminals are caused by other possible solutions that satisfy the terminal compositions and may be amended by including multiple diffusion couplings. We also note the relative errors at the interface rise to around 20%. Such deviation is largely due to the simulation errors of the numerical scheme first used to generate the synthetic (measurement) data and then used to construct the composition-distance curve once the inter-diffusivity coefficients are determined via compressed sensing. Independent from the CS framework, those errors would decrease should one have employed high-order numerical schemes, such as the finite element method of local discontinuous Galerkin, and/or with a more refined grid. However, this is beyond the focus of the current study and will be addressed in future works.

3.4. Discussions

Compressed sensing method works well when there is fewer data than unknowns. As a rule of thumb, one may select the number of measurement points with a minimum of $\frac{1}{3} n \times size(\mathbf{a})$ and a maximum of $\frac{2}{3} n \times size(\mathbf{a})$, in which $\mathbf{a}$ is the unknown vector of functional coefficients and n is the number of our coupled Boltzmann-Matano diffusion equations. For example, in the ternary system, the minimum number of measurement points is $1, 2$ and 4 for a zeroth-, first- and second-order polynomial representation of inter-diffusivity, respectively. In the quaternary system, the corresponding minimum number becomes $1, 4, 7$ for the zeroth-, first- and second-order polynomial representations, respectively. These numbers are at least representative of, sometimes less than the amounts one may encounter in experiments.

In addition to the time-consuming process of EPMA experiments, measurement data is prone to errors mainly from its analysis step. It is usually believed that the experimental uncertainty of EPMA is within 2% in a quantitative analyzation mode. In our numerical examples, such experimental errors are represented by those resulting from the numerical scheme used to obtain the synthetic data. For measurements of strength σ, the ℓ_2 estimation error from compressed sensing can be summarized as [26]:

$$|\epsilon|_{\ell_2} = \text{polylog}(n) \frac{s}{m} \sigma^2, \tag{25}$$

where n is the size of unknown vector, s represents the number of nonzero entries and m is the number of data entries. A more thorough study on the compressed sensing method using experimental data is beyond the scope of this study but would be addressed in future works.

As shown in the examples, no definite answer is given on the exact locations of measurements $c(x)$ on the composition-distance curve, as long as they are in the diffused zone. Hence the solution vector of inter-diffusion coefficients from compressed sensing is non-unique, an inherent nature of inverse problems. However, in the context of diffusion modeling, those solutions are "effective" as long as they provide good estimations on the composition-distance curve.

It is also noted here that for our compressed sensing framework, sufficient conditions to ensure that the ℓ_1-regularized system indeed has a well-defined solution are known [31]; practical sampling conditions to ensure this well-posed property often rely on randomized sampling [32], which is also why we utilize random sampling for this procedure.

Lastly, the nature of compressed sensing is to obtain a solution (of coefficients) matrix as sparse as possible. In other words, it provides a mean to modify the "pre-selected" order of the polynomial expression of inter-diffusivity as a function of compositions, in order to approach the actual expression by eliminating the excessive coefficients.
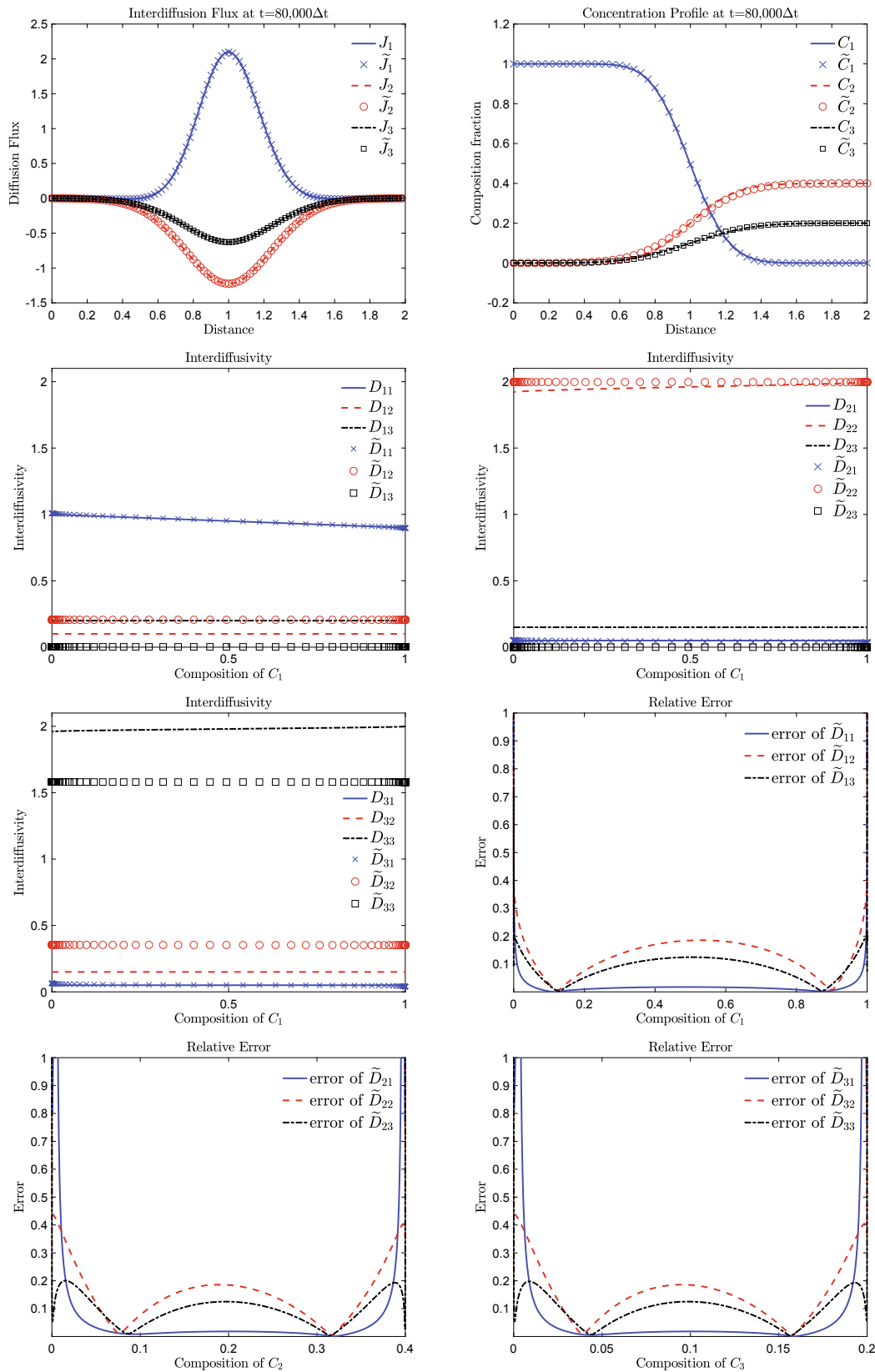
Fig. 3. Benchmark solutions and results from compressed sensing on: (a) inter-diffusion fluxes, (b) concentration profile, (c), (d) & (e) diffusion coefficients and their relative error (10) with respect to composition (f) c_1, (g) c_2 and (h) c_3, respectively, in the case of 1st-order inter-diffusivities for quandary system.

4. Conclusion

In this paper, we propose a novel numerical method to estimate the inter-diffusivity coefficients. Using the Boltzmann-Matano equations as predictive tools, our inverse framework employs compressed sensing to extract the diffusion coefficients from a small number of samples on the composition-distance curves. Through three numerical examples, we come to the following conclusions: Our method provides excellent estimations of the inter-diffusivity coefficients and good recovery of the composition-distance curve. It requires less data than the conventional methods based on a least-squares approach as long as the solution vector is sufficiently sparse. The user must provide a plausible ansatz for the functional relationship between the diffusion coefficients and concentrations, but the new method does not impose any additional *a priori physical or modeling assumptions about this functional relationship. Our procedure also does not impose any preference on the locations of the samples, as long as they lie in the diffused zone, and the procedure is applicable to an arbitrary number of species. Finally, it provides a means to select and eliminate the order of the polynomial expression of inter-diffusivity as a function of compositions.*

However, the problem of recovering inter-diffusivity predictions from concentrations is an ill-posed inverse problem, and so many solutions exist. The proposed method can recover relationships whose functional structure can be sparsely represented in a user-prescribed basis; while this representation is not necessarily the "correct" relationship, it does choose an "effective" relationship that correctly predicts concentrations. The accuracy of our approach at the terminal compositions could be enhanced if concentration curve data from multiple couplings with different composition angles are used, and the inter-diffusivity coefficients are described with a single set of adjustable parameters. Lastly, physical constraints such as positivity of the inter-diffusion coefficients can be incorporated in future inverse frameworks.

Data availability

The raw/processed data required to reproduce these findings cannot be shared at this time as the data also forms part of an ongoing study.

CRediT authorship contribution statement

Yi Qin: Investigation, Funding acquisition, Validation, Writing - original draft. **Akil Narayan:** Investigation, Methodology, Writing - original draft. **Kaiming Cheng:** Conceptualization, Methodology, Supervision, Funding acquisition, Writing - original draft. **Peng Wang:** Conceptualization, Methodology, Supervision, Funding acquisition, Visualization, Writing - original draft.

Declaration of Competing Interest

The authors declare that they have no known competing financial interests or personal relationships that could have appeared to influence the work reported in this paper.

References

[1] A. Fick, Ueber diffusion, Pogg. Ann. 94 (1855) 59–86.

[2] L. Onsager, Theories and problems of liquid diffusion, Ann. N.Y. Acad. Sci. 46 (1945) 241–265.

[3] J.S. Kirkaldy, J.E. Lane, G.R. Mason, Diffusion in multicomponent metallic systems: Vii. solutions of the multicomponent diffusion equations with variable coefficients, Can. J. Phys. 41 (1963) 2174–2186.

[4] L. Boltzmann, Zur integration der diffusionsgleichung bei variabeln diffusionscoefficienten, Ann. Phys. 53 (1894) 959–964.

[5] C. Matano, On the relation between diffusion-coefficients and concentrations of solid metals, Jpn. J. Phys. 8 (1933) 109–113.

[6] M.A. Dayananda, Y.H. Sohn, A new analysis for the determination of ternary interdiffusion coefficients from a single diffusion couple, Metall. Mater. Trans. A 30 (1999) 535–543.

[7] J. Cermak, V. Rothova, Concentration dependence of ternary interdiffusion coefficients in ni3al/ni3al–x couples with x= cr, fe, nb and ti, Acta. Mater. 51 (2003) 4411–4421.

[8] A. Paul, A pseudobinary approach to study interdiffusion and the kirkendall effect in multicomponent systems, Philos. Mag. 93 (2013) 2297–2315.

[9] A. Dash, N. Esakkiraja, A. Paul, Solving the issues of multicomponent diffusion in an equiatomic nicofecr medium entropy alloy, Acta Mater. 193 (2020) 163–171.

[10] N. Esakkiraja, A. Gupta, V. Jayaram, T. Hickel, S.V. Divinski, A. Paul, Diffusion, defects and understanding the growth of a multicomponent interdiffusion zone between pt-modified b2 nial bond coat and single crystal superalloy, Acta Mater. 195 (2020) 35–49.

[11] R. Bouchet, R. Mevrel, A numerical inverse method for calculating the interdiffusion coefficients along a diffusion path in ternary systems, Acta Mater. 50 (2002) 4887–4900.

[12] J. Andersson, J. Ågren, Models for numerical treatment of multicomponent diffusion in simple phases, J. Appl. Phys. 72 (4) (1992) 1350–1355.

[13] W. Chen, L. Zhang, Y. Du, C. Tang, B. Huang, A pragmatic method to determine the composition-dependent interdiffusivities in ternary systems by using a single diffusion couple, Scr. Mater. 90–91 (2014) 53–56.

[14] Q. Zhang, J. Zhao, Extracting interdiffusion coefficients from binary diffusion couples using traditional methods and a forward-simulation method, Intermetallics 34 (2013) 132–141.

[15] K. Cheng, W. Chen, D. Liu, L. Zhang, Y. Du, Analysis of the cermak–rothova method for determining the concentration dependence of ternary interdiffusion coefficients with a single diffusion couple, Scr. Mater. 76 (2014) 5–8.

[16] K. Cheng, J. Zhou, H. Xu, S. Tang, Y. Yang, An effective method to calculate the composition-dependent interdiffusivity with one diffusion couple, Comput. Mater. Sci. 143 (2018) 182–188.

[17] K. Cheng, H. Xu, B. Ma, J. Zhou, S. Tang, Y. Liu, C. Sun, N. Wang, M. Wang, L. Zhang, Y. Du, An in-situ study on the diffusion growth of intermetallic compounds in the al–mg diffusion couple, J. Alloys Compd. 810 (2019), 151878.

[18] K. Cheng, J. Sun, H. Xu, J. Wang, C. Zhan, R. Ghomashchi, J. Zhou, S. Tang, L. Zhang, Y. Du, Diffusion growth ϕ ternary intermetallic compound in the mg-al-zn alloy system: in-situ observation and modeling, J. Mater. Sci. Technol. in press.

[19] A. Paul, T. Laurila, V. Vuorinen, S.V. Divinski, Thermodynamics, Diffusion, and the Kirkendall Effect in Solids, Springer International Publishing, Cham, 2014.

[20] D.L. Donoho, For most large underdetermined systems of linear equations the minimal 1-norm solution is also the sparsest solution, Commun. Pure Appl. Math. 59 (6) (2006) 797–829.

[21] E.J. Candes, J. Romberg, T. Tao, Robust uncertainty principles: exact signal reconstruction from highly incomplete frequency information, IEEE Trans. Inf. Theory 52 (2) (2006) 489–509.

[22] E.J. Candès, J.K. Romberg, T. Tao, Stable signal recovery from incomplete and inaccurate measurements, Commun. Pure Appl. Math. 59 (8) (2006) 1207–1223.

[23] E. Candes, J. Romberg, l1-magic: Recovery of sparse signals via convex programming, URL: www. acm. caltech. edu/l1magic/downloads/l1magic. pdf 4 (2005) 14.

[24] E.V. Berg, M. Friedlander, Spgl1: A solver for large-scale sparse reconstruction, see http://www. cs. ubc. ca/labs/scl/spgl1.

[25] J.F. Sturm, Using sedumi 1.02, a matlab toolbox for optimization over symmetric cones, Optim. Method Softw. 11 (1–4) (1999) 625–653.

[26] Y. Plan, Compressed sensing, sparse approximation, and low-rank matrix estimation, Ph.D. thesis, California Institute of Technology, 2011.

[27] J.S. Kirkaldy, D.J. Young, Diffusion in the condensed state, The Institute of Metals, 1 Carlton House Terrace, London SW1Y 5DB, UK, 1987.

[28] W. Hopfe, J. Morral, Uncertainty analysis of ternary diffusivities obtained from one versus two compact diffusion couples, J. Phase Equilib. Diff. 37 (2) (2016) 110–118.

[29] J. Morral, W. Hopfe, Validation of multicomponent diffusivities using one diffusion couple, J. Phase Equilib. Diff. 35 (6) (2014) 666–669.

[30] H. Xu, K. Cheng, J. Zhong, X. Wu, M. Wei, L. Zhang, Determination of accurate interdiffusion coefficients in fcc ag-in and ag-cu-in alloys: A comparative study on the matano method with distribution function and the numerical inverse method with hitdic, J. Alloys Compd. 798 (2019) 26–34.

[31] A. Cohen, W. Dahmen, R. DeVore, Compressed sensing and best k-term approximation, J. Am. Math. Soc. 22 (1) (2009) 211–231, https://doi.org/10.1090/S0894-0347-08-00610-3.

[32] H. Rauhut, Compressive Sensing and Structured Random Matrices: in: M. Fornasier (Ed.), Theoretical Foundations and Numerical Methods for Sparse Recovery, 2010, pp. 1–92. URL: http://www.degruyter.com/view/books/9783110226157/9783110226157.1/9783110226157.1.xml.